Nuclear Materials and Energy 37 (2023) 101514

Contents lists available at ScienceDirect

Nuclear Materials and Energy

journal homepage: www.elsevier.com/locate/nme

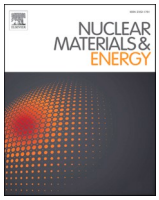

Performance of tungsten plasma facing components in the stellarator experiment W7-X: Recent results from the first OP2 campaign

Dirk Naujoks [a,*], Chandra-Prakash Dhard [a], Yuhe Feng [a], Yu Gao [a], Torsten Stange [a], Birger Buttenschön [a], Sergey A. Bozhenkov [a], Sebastijan Brezinsek [b], Kai Jakob Brunner [a], Gábor Cseh [c], Andreas Dinklage [a], David Ennis [d], Joris Fellinger [a], Eric Flom [a], Dorothea Gradic [a], Eduard Grigore [e], Dirk Hartmann [a], Frederik Henke [a], Marcin Jakubowski [a], Amit Kharwandikar [a], Mikhail Khokhlov [a], Jens Knauer [a], Gábor Kocsis [c], Petra Kornejew [a], Maciej Krychowiak [a], Matej Mayer [f], Paul McNeely [a], Daniel Medina [g], Rudolf Neu [f], Kian Rahbarnia [a], Cristian Ruset [e], Norbert Rust [a], Peter Scholz [a], Thomas Sieber [a], Ivan Stepanov [a], Naoki Tamura [h], Erhui Wang [b], Thomas Wegner [a], Daihong Zhang [a], the W7-X Team [1]

[a] *Max-Planck-Institut für Plasmaphysik, Wendelsteinstraße 1, 17491 Greifswald, Germany*
[b] *Forschungszentrum Jülich GmbH, Institut für Energie- und Klimaforschung, Plasmaphysik, 52425 Jülich, Germany*
[c] *Atomic Energy Research Institute, 29-33. Konkoly-Thege Miklós út, Budapest 1121, Hungary*
[d] *Department of Physics, Auburn University, 380 Duncan Drive, Auburn, AL 36849, USA*
[e] *National Institute for Laser, Plasma and Radiation Physics, P.O. Box MG-36, Magurele-Bucharest, Romania*
[f] *Max-Planck-Institut für Plasmaphysik, Boltzmannstr. 2, 85748 Garching, Germany*
[g] *Laboratorio Nacional de Fusión, CIEMAT, Av. Complutense 40, 28040 Madrid, Spain*
[h] *National Institute for Fusion Science, National Institutes of Natural Sciences, Toki 509-5292, Japan*

ARTICLE INFO

Keywords:
Stellarator W7-X
Plasma facing components
Tungsten materials

ABSTRACT

The transition to reactor-relevant materials for the plasma facing components (PFCs) is an important and necessary step to provide a proof of principle that the stellarator concept can meet the requirements of a future fusion reactor by demonstrating high performance steady-state operation. As a first step to gain experience with tungsten as plasma-facing material in the Wendelstein 7-X (W7-X) stellarator, graphite tiles coated with an approximately 10 μm MedC tungsten layer (NILPRP Bucharest) were installed to complete the ECRH beam dump area in two of the five plasma vessel modules over an area of approximately one square meter each. In addition, tungsten baffle tiles are installed (40 tiles in total) with either bulk tungsten as part of NBI shine-through target or with a tungsten heavy alloy (W95-Ni3.5-Cu1.5) to replace the graphite tiles that were previously thermally overloaded. Based on an advanced diffusive field line tracing method and EMC3-Eirene simulations, the overloaded baffle tiles were redesigned by making the tiles thinner (i.e. moving the plasma-facing surface (PFS) away from the hot plasma region) and by reducing the local angle of incidence through toroidal displacement of the watershed. Significant erosion of the tungsten tiles can only be expected if sputtering by impurity ions such as carbon or oxygen ions contributes. However, the resulting central concentration of tungsten and the corresponding radiation losses are expected to be marginal. The expected deposition of carbon on the tungsten surfaces in the baffle regions mitigates further the possible tungsten enrichment in the core plasma. In OP2.1, no adverse effects of the installed tungsten PFCs on the plasma performance were observed during normal plasma operation. With the design changes made in the baffle area, the predicted heat load reductions could be experimentally confirmed.

* Corresponding author.
E-mail address: dirk.naujoks@ipp.mpg.de (D. Naujoks).
[1] The full list of W7-X Team members is given in T. Sunn Pedersen et al 2022 Nucl. Fusion 62 042022.

https://doi.org/10.1016/j.nme.2023.101514
Received 30 June 2023; Received in revised form 15 September 2023; Accepted 18 September 2023
Available online 19 September 2023

Introduction

During the experimental programs with the stellarator experiment W7-X, starting with the first operation phase OP1.1 (Dec. 2015 – March 2016, with five graphite limiters on the inner wall, 5 MW ECRH, 4 MJ energy input) [1] up to OP1.2a (Sept. 2017 – Dec. 2017) [2] and OP1.2b (July 2018 – Oct. 2018, with Test Divertor Units (TDU), 8 MW ECRH, 200 MJ energy input) [3], the energy input and plasma performance as well as the heat and particle loads on the in-vessel components have been continuously increased. Except for the poloidal closure and the wall panels (stainless steel plates), all other components are covered with fine-grain graphite tiles. During this phase, only some parts of the first wall (beam dumps of the Neutral Beam Injection (NBI), cooling loops of the glow discharge electrode housing) were water-cooled.

During the subsequent completion phase, the originally installed TDUs were replaced with the water-cooled High Heat Flux Divertor (HHF-Divertor, with carbon fiber composite (CFC) target elements [4]) together with a cryo-vacuum pump system; one cryopump in each of the 10 divertor units [5]. Actively cooled port liners were installed at selected ports that might otherwise be overloaded by plasma and stray radiation of the Electron Cyclotron Resonance Heating (ECRH) system. Nearly all plasma facing components (except some diagnostic systems, which are still to be upgraded) were designed for OP2 to be water-cooled to withstand the power and particle exhaust during full power discharges under steady-state conditions. A description of the first wall components of W7-X (divertor units with poloidal and toroidal closures, pump gap protection, baffle and heat shield modules, wall panels, port protections, protective housings for diagnostics, cryopumps) as well as their specified limits is given in [4].

After completion, the operation phase OP2.1 (Sep. 2022 – March 2023) was successfully carried out, achieving the target of 1 GJ operation in terms of input power (1.3 GJ in program XP_20230215.32, 8 min duration, max. 3 MW ECRH power). The development and demonstration of this long-pulse operation (1 GJ energy turnaround) without overloading the plasma facing components is one of the main results of the campaign. Under detached conditions, large reduction of the convective heat fluxes to the divertor targets (an order of magnitude less than those of attached plasmas) could be achieved by increasing the line-integrated density up to 1.4×10^{20} m^{-2} (program XP_20230222.16), even without using seeding impurities, resulting in radiated power fractions of 85% or more. Stable (power) detachment with Ne seeding has been demonstrated with a pulse duration of 110 s (program XP_20230209.23).

Parallel to the preparation of OP2.1, intensive discussions on the necessary extensions for W7-X were held in the framework of special workshops organized by IPP Greifswald and the internal temporary working group "W7-X Strategy 2030", with the participation of external experts. Two main objectives have been identified and discussed with regard to the required resources and detailed implementation options: the increase of the plasma heating power and the transition to an all-metal plasma facing components device. It is generally agreed that the reactor relevance of any magnetic confinement fusion concept requires operation with all-metal plasma facing components (PFC), as also expressed in the European fusion roadmap for the development of the stellarator reactor line. The transition to metallic PFCs for the W7-X stellarator represents a long and resource-intensive activity which should begin with the complete removal or coating of the carbon tiles on the heat shield and baffle modules before the divertor units could be replaced with a new tungsten divertor. Several options were discussed, including reusing the inertially cooled TDUs for a faster, less expensive implementation by replacing the graphite with tungsten elements. Besides the resulting problems for the integration of the new cryopumps installed before OP2.1, a counter argument is the incompatibility of an uncooled divertor with the load specification of W7-X, which aims at high steady-state heat loads of 10 MW/m^2 for at least 30 min (18 GJ goal). Partial replacement of individual target modules was also judged not to be justified by the same consideration, and would also limit the current operational flexibility by using the magnetic field configuration space of W7-X.

In-situ, direct W coating of the components installed in the plasma vessel, including the CFC divertor targets, could be a very promising technique, as it could avoid lengthy and expensive assembly operations and long downtimes. Therefore, the development of in-situ coating techniques that address both the surface morphology and the surface processing and finishing of W7-X plasma components is considered a valuable part of the IPP strategy to transform W7-X into a carbon-free device. In particular, their application as a potential repair technology for tungsten-based plasma cladding components in W7-X would contribute significantly to keep the downtime acceptable in case of potential damage during the upcoming plasma operation with an energy input of up to 18 GJ. These advanced coating techniques, based on plasma spray methods, are currently being developed at FZ Jülich. Progress towards a qualified technology will be reviewed as part of the tungsten divertor design review process. In-situ wall coating techniques, such as glow discharge operation with WF_6 injection [6], are not pursued because of the expected inhomogeneous distribution of the deposited tungsten layers; the corresponding safety and technical measures would be quite demanding to prevent damage to components by hydrofluoric acid as by-product.

The above mentioned options would imply to keep the current plasma-facing surface (PFS) of the divertor targets and baffles. Although excellent stellarator performance could be achieved with the OP1.2b setup, some design weaknesses were discovered which led to operational limitations: certain baffle modules and in particular the central horizontal area of the divertor targets (TM5h, TM6h) were loaded above their specified thermal loads. In addition, only relatively low neutral gas pressures in the sub-divertor space and thus reduced particle removal could be achieved: sufficient for plasma density control even during longer discharges of several minutes, but not efficient enough to be able to compensate sufficiently for additional sources such as steady-state pellet injection under saturating/outgassing wall conditions in future campaigns. Therefore, a new design of the divertor components with a redefined PFS is envisaged, aiming at tolerable thermal loads, high particle exhaust and sufficient impurity control [7]. In early 2021, the development and qualification of target elements with tungsten-based armor material (W or W heavy alloys) with a load specification of 10 MW/m^2 in steady-state operation was started in the framework of EUROfusion. It is being investigated whether the 3D shape requirements for the plasma-facing surface of the target elements in W7-X can be met by using single flat-tile elements with rather limited 3D topology shaping capabilities [8]. The use of steel components instead of plasma-facing graphite components could be an option for low load areas on the first wall. Based on the PFS definition and the target element design, the integrated design phase will follow accompanied by international reviews.

As a first step towards a carbon-free W7-X device, areas of several square meters have been equipped with tungsten as plasma-facing material: graphite tiles with a tungsten coating in the heat shield area as well as pure tungsten and tungsten alloy tiles in a specific baffle module (BM1v, v - vertical), as described in Sect. 2. In addition, tungsten-coated tiles were placed at positions of the inner heat shield with good spectroscopic coverage to allow a comparison of tungsten and graphite materials. Special marker layer tiles were used for long-term exposure; ex-situ surface analyses will be conducted after the completion of the campaign (Section 2.3). The effect of the installed tungsten PFCs on the overall plasma performance in the first plasma experiments (OP2.1) with an active water-cooled high-heat flux divertor is reported by evaluating its compatibility with high-power, long-pulse operation in W7-X (Section 3). In particular, the implications of using tungsten components in the ECRH (Section 2.1) and NBI beam dump areas (Section 2.2) and the associated risks of possible excessive tungsten erosion are discussed.

Tungsten PFCs in the stellarator W7-X and OP2.1 results

Experience with the use of graphite materials in W7-X has been gained now in four campaigns [9,10] and shows the known advantages: Carbon has excellent thermo-physical properties, shows no melting, has high thermal shock resistance, and keeps its shape even under extreme temperature variations. Once emitted by erosion processes, carbon serves as an effective radiator in the edge plasma. However, the associated disadvantages have also been demonstrated: Even at low energies (a few eV) and at room temperature, carbon is eroded by the formation of volatile hydrocarbons at relatively high erosion rates. Thick layers of hydrogenated carbon films are deposited on all plasma facing components [9], as well as on components in remote areas. These layers, which tend to flake off, contain large amounts of hydrogen isotopes. The ability to co-deposit tritium prevents the use of carbon in future fusion reactors.

The use of high-Z materials has been strictly avoided for years after the first bad experiences at the beginning of fusion research. A tiny concentration in the plasma center is enough to extinguish the plasma by radiation. The development of plasma scenarios with a rather cold edge and the use of divertors brought materials such as tungsten back into consideration. Starting with the exposure of small probes made of high-Z materials [11], ASDEX-Upgrade, for example, now operates with wall and divertor plates completely covered by tungsten without significant degradation of plasma performance at high density [12]. An issue of concern is the often observed phenomenon of high-Z enrichment/accumulation, which could be particularly critical for stellarators. A stepwise increase of the areas covered with tungsten PFCs is planned in W7-X in order to study possible detrimental effects of tungsten as a high-Z material on the plasma operation in W7-X and to develop appropriate plasma scenarios to mitigate operational limitations.

Heat shield area (ECRH beam dump)

In OP1.2b, no evidence of tungsten enrichment in the core plasma was found – after installation of 10 TZM (TZM: Mo alloy with 0.5 wt% Ti, 0.1 wt% Zr) reflector tiles covered with a 10 μm tungsten layer as part of the ECRH beam dump area, 21 graphite tiles with W coating (tungsten layer of about 50–200 nm and installed at different positions in all W7-X modules, the scraper elements with W marker layers, as well as 3 tiles of a target element (PWI finger TM2h6) of the TDU19 coated with a thin tungsten marker layer at strike line positions with strong net erosion [9,10]. Even in the experiment where the target heat loads were toroidally asymmetrically concentrated on the divertor unit with the W-coated element for the special overload experiment, no tungsten was seen spectroscopically.

In preparation for OP2.1, 200 tiles were installed in the heat shield area to complete the ECRH beam dump in the plasma vessel modules 1 and 5. This includes 18 tungsten-coated TZM tiles (16 new and 2 from OP1.2b) and 24 tungsten-coated graphite tiles, four of which serve as reflector tiles during the ECRH operation. Several investigations and tests have been conducted on various W-heavy alloys for use as plasma-facing material, see [13,14].

The ECRH second harmonic O-mode heating scenario (O2-ECRH), which enables plasma operation with line averaged densities $n_{e,\,dl}$ in the range from $8x10^{19}$ up to $1.4x10^{20}$ m^{-2} [15], has been redesigned for OP2 to reduce the stray radiation level by about 50% by using these special reflector tiles (Fig. 1).

The surface of the tiles is prepared with special gratings to allow to control the beam direction and polarization of the second pass through the plasma to increase the overall microwave absorption.

All 200 tiles (graphite and TZM) were coated with an approximately 10 μm thick MedC tungsten layer using a combined magnetron sputtering and ion implantation method developed by NILPRP Bucharest [16]. Another purpose of the use of tungsten plasma facing components

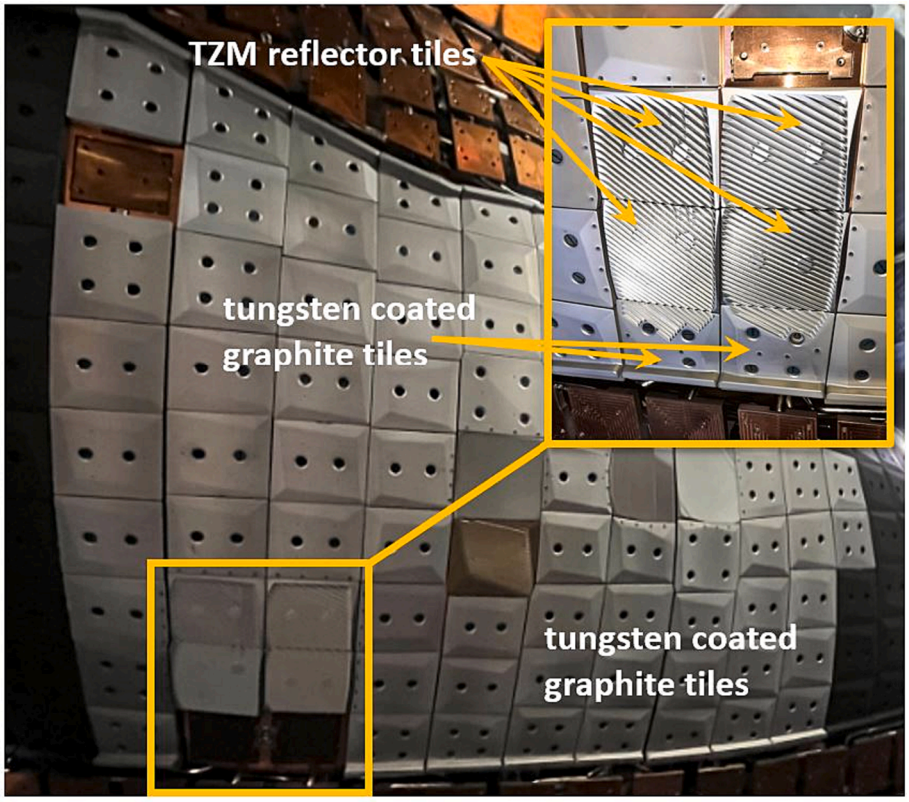

Fig. 1. Tungsten-coated heat shield tiles in the ECRH beam dump areas (about 1 m^2 each in the plasma vessel modules 1 and 5). At the top right, reflector tiles with special reflection gratings are shown in an enlarged view.

is to improve the wall reflectivity for microwaves (by a factor of 10 compared to graphite surfaces), thus promoting multi-pass plasma absorption in O2 operation under high plasma density conditions ($n_{e,dl} > 8{\cdot}10^{19}$ m^{-2}). Eight of the coated metal reflector tiles had to be stripped of the tungsten coating by glass bead blasting prior to being mounted on the heat shield, because local delamination was observed during quality control on the grating surface and partially on the side of these tiles. As a risk mitigation measure it was then decided to remove these coatings. The problem may be related to the fact that the standard surface preparation process, which includes appropriate grinding, could not be carried out to the extent necessary to avoid damaging the special grating surface. To be on the safe side, these metal reflector tiles will no longer be coated in the future, because plasma contamination with molybdenum was not observed in OP2.1. This reduces cost and schedule risk. Furthermore, there is no risk of delamination during plasma operation. The condition of the coating on the other installed tiles will be checked during the visual inspection when the plasma vessel is opened for access. No damage is expected, as this type of coating has shown high reliability not only in W7-X in previous campaigns, but also in other fusion experiments.

During OP2.1, there was only one case where strong emission of tungsten particles and clusters was observed during the plasma operation. In this particular case (W7-X program number: XP_20221207.58), the NBI operation induced the formation of peaked profiles leading to a stronger refraction of the ECRH beam, as expected from the OP1.2b experience. The ECRH beam (operated in O2-heating mode) did not hit the center of one of the intended reflector tiles, but hit a gap between a metal reflector tile and an adjacent tungsten-coated carbon tile. This led to local arcing, resulting in a strong tungsten emission with release of larger tungsten pieces/flakes/clusters as seen in the video monitoring, and finally to the termination of the plasma discharge with a complete loss of the plasma diamagnetic energy within 110 ms. With appropriate adjustments in the operation of the ECRH heating system, further incidents could be prevented in the campaign.

In general, central ECRH heating has been found to be useful in keeping the concentration of impurity ions in the core plasma low, where peak profiles during NBI heating result in longer particle confinement times, similar to observations in the ASDEX Upgrade tokamak [17].

Baffle area (part of NBI beam dump in plasma vessel module 2)

At positions in the baffle areas (BM1v vertical baffle modules), where excessive thermal loads were observed during OP1.2b in the high-mirror and standard configurations [18], graphite tiles were replaced by tungsten tiles (W95-Ni3.5-Cu1.5-alloy as well as pure tungsten) with modified geometry (reduced thickness). These baffle modules were fitted with bulk tungsten (as part of the NBI beam shine through areas in module 2) and tungsten heavy alloy tiles (W95-Ni3.5-Cu1.5) in the other plasma vessel modules – 40 tiles in total. Based on diffusive field line tracing and EMC3-Eirene simulations, a modified plasma-facing surface was defined [19] and implemented for these particular ten BM1v baffle modules by making the tiles thinner (i.e. moving the PFS away from the hot plasma region) and by reducing the local angle of incidence by toroidal displacement of the watershed (Fig. 2).

A system for quick termination of the NBI beam is required for safe operation of W7-X. Determining the surface temperature of the wall elements in the beam dump area is essential. The use of tungsten tiles on the baffle raised some issues for the Heat Shield Thermography (HST) safety system and the operation of the NBI. The W7-X NBI system is described in [20]. IR observation of tungsten surfaces is much more difficult and error prone than that of carbon surfaces. For this reason, the line of sight of the HST pyrometers of both sources 3 and 7 was moved to the adjacent carbon tile. ANSYS calculations show that the surface

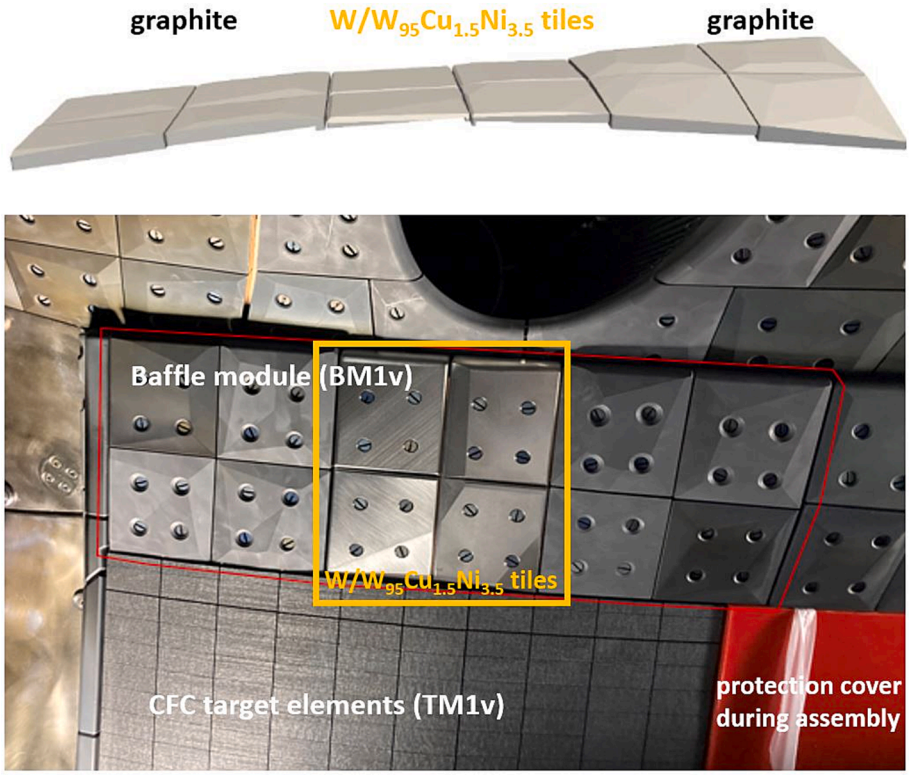

Fig. 2. View of one of the 10 BM1v baffle modules (marked by the red rectangle) with the tungsten tiles (pure W (in module 2), W95Ni3.5Cu1.5 in the plasma vessel modules 1, 3, 4, 5) in the center position (indicated by the yellow rectangle). This particular photo was taken in plasma vessel module 1, lower divertor with 4 WNiCu tiles in the center of this baffle module. Above, a side CAD view of BM1v shows the thickness variation for the different tungsten and modified graphite tiles. (For interpretation of the references to colour in this figure legend, the reader is referred to the web version of this article.)

temperature of this carbon tile can be used to trigger beam termination to safeguard the beam dump area. In addition, the thermo-mechanical calculations clearly show that reducing the thickness of the carbon tile to match the thickness of the new tungsten tiles causes a significant, but fortunately noncritical, temperature increase of both the carbon surface and the Cu-Cr-Zr heat sink. In OP2.1 the HST system worked successfully for source 7. Unfortunately, the calculations for the tungsten baffle tiles show a substantial temperature rise in the Cu-Cr-Zr heat sink during long NBI operation due to a high thermal transfer rate from the tungsten to the heat sink. This may be a limitation for future planned long pulse operation of the NBI.

If the whole beam dump area is made of tungsten in the future, it will not be possible to adjust the HST line of sight as was currently possible. Therefore, both a solution for accurate IR surface temperature measurement and optimization of the tungsten tile design, taking into account NBI power loads of up to 16 MW/m^2, are necessary for the future use of tungsten in the beam dump area.

The aim of specific experimental investigations in OP2.1 was to determine whether and to what extent the modified design (Fig. 2) leads to a reduction of the heat loads. A comparison of the obtained mean heat loads and maximum heat flux densities for similar discharges (using the high-mirror magnetic field configuration) performed in OP1.2b (with the old design) and in OP2.1 (with the modified tiles) is given in Table 1.

Two different ECRH heating powers are considered: a) $P_{ECRH} = 3$ MW with a line-integrated plasma density $n_{e,\ dl} = 4.5\text{-}5{\cdot}10^{19}$ m^{-2}, plasma diamagnetic energy $W_{dia} = 0.3$–0.4 MJ, plasma radiation losses $P_{rad} = 0.5$–0.8 MW and b) $P_{ECRH} = 5$ MW with a line integrated plasma density $n_{e,\ dl} = 6{\cdot}10^{19}$ m^{-2}, plasma diamagnetic energy $W_{dia} = 0.4$–0.5 MJ, plasma radiation losses $P_{rad} < 1$ MW. The values for the mean heat loads have been obtained by integrating over 8 central tiles of BM1v, i.e. including the 4 tungsten material tiles and 2 adjacent graphite tiles to the left and right of them. Fig. 3 shows the spatial distribution of the surface temperatures as measured by the IR thermography [21] and the evaluated heat flux densities for the 5 MW case. With the new OP2.1 design, a reduction of both the peak heat flux and heat load by a factor of 2–3 could be demonstrated. The emissivity of tungsten is assumed to be 0.67 based on the equilibrium temperature of 50 °C during the IR thermography test measurements by heating up the target and baffle water circuits to this temperature. Note: Much lower values would be expected for a tungsten surface (see discussion in Sect. 3.2).

Special tiles for spectroscopy and ex-situ surface analysis

In addition to the modifications described above, tungsten-coated graphite tiles were placed at positions on the inner heat shield with good spectroscopic coverage to allow a direct comparison of the recycling behavior on graphite and tungsten surfaces. These investigations could not be completed in OP2.1 and will be continued in the upcoming campaigns OP2.2/OP2.3 (2024/2025).

16 coated tiles with special marker layers are also installed in the plasma vessel modules 1 and 5 as long-term samples with the following structure: graphite as substrate material, a Mo interlayer 2–3 μm thick, a tungsten coating with a thickness of about 10 μm, an additional Mo interlayer 500 nm thick and finally on top a 100 nm thick tungsten coating. These tiles will be removed after opening the plasma vessel in summer 2023 and used for ex-situ surface analysis to study in detail the effect of erosion by charge exchange neutrals and deposition of intrinsic carbon impurities. In particular, the erosion of the PFCs on the wall due to the impact of energetic neutrals is still an open question regarding its relevance in the W7-X stellarator experiments.

Several material samples were prepared for exposure with the Multi-Purpose Manipulator (MPM) [22], unfortunately, this could not be realized in OP2.1; these studies on material erosion, deposition and migration will be postponed to the next experiment campaigns.

Assessment of tungsten erosion and core concentration

This section presents estimates of the different erosion processes and derives the corresponding core concentrations to answer the question of whether the diagnostic systems available at W7-X would, in principle, be sensitive enough to detect tungsten once it has been eroded and transported into the edge and core plasma.

Tungsten erosion by plasma ions, charge-exchange neutrals, and NBI beam

Tungsten shows negligible erosion by hydrogen isotopes at low plasma temperatures, i.e., at low ion impact energies. However, erosion by impurity ions and by fast particles from additional heating, e.g. using neutral beam injection or ICRH can be a problem. The effects of self-sputtering, redeposition and sticking can be considered by introducing an effective sputtering yield Y_{eff} [23]

$$Y_{eff} = \frac{\left(1 - sP_{redep}\right)\sum_i Y_i f_i}{1 - P_{redep}\left(Y_{self} + 1 - s\right)} \tag{1}$$

If the sticking coefficient of the redeposited material s and the redeposition probability P_{redep} are close to unity, the effective sputtering will be small. Excessive sputtering can be initiated with a large self-sputtering yield Y_{self}; if $P_{redep}(Y_{self} + 1 - s) \geq 1$, then runaway erosion occurs. In the case of $s = 1$ and $Y_{self} = 0$, the erosion flux density Γ_{ero} simply becomes

$$\Gamma_{ero} = \Gamma_e Y_{eff} = \Gamma_e (1 - P_{redep}) \sum_i Y_i f_i \tag{2}$$

where the electron flux density is given by $\Gamma_e = n_e c_s \sin\alpha$; with the angle of incidence of the magnetic field lines α, the electron density at the target n_e, and the ion sound speed c_s. This erosion flux is obtained by the erosion due to all plasma ions, including all impurity ions with their corresponding sputtering yields Y_i and concentration f_i related to the electron density. Prompt redeposition of emitted tungsten atoms is rather high in the case of direct plasma contact, where close ionization occurs. However, tungsten atoms emitted from wall elements such as the heat shield or baffle areas have to overcome the relatively large distance to hot plasma regions, as they are likely to be ionized only close to the separatrix. In this case, the large gryoradius of the tungsten ions does not lead to a prompt redeposition during their gyration, since the wall would be too far away. Considering wall erosion, the effect of prompt redeposition can, therefore, be neglected, $P_{redep} = 0$.

The sputtering yield of tungsten bombarded by hydrogen ions is about $Y_{H+\rightarrow W} \simeq 10^{-5}$ [11] assuming a plasma temperature of 30 eV. This takes into account the Maxwellian distribution of the plasma ions as well as the acceleration of the ions in the electric sheath. However, erosion by carbon impurities could significantly increase the tungsten erosion, e.g.

Table 1
Comparison of the heat loads on the baffle module BM1v for the different designs as used in the experiment campaign OP1.2b (graphite tiles) and OP2.1 (4 thin tungsten/ W95Ni3.5Cu1.5 tiles together with adjacent graphite tiles reshaped to ensure smaller angles of incidence) and for two different ECRH heating powers (3 MW, 5 MW). The corresponding discharges are given with their program number.

	XP_20181011.21 (OP1.2b: 5 MW)	XP_20230328.23 (OP2.1: 5 MW)	XP_20181009.09 (OP1.2b: 3 MW)	XP_20230328.33 (OP2.1: 3 MW)
Mean heat load [kW/m^2]	129.7	81.8	82.8	47.1
Max heat flux [MW/m^2]	0.95	0.3	0.92	0.26

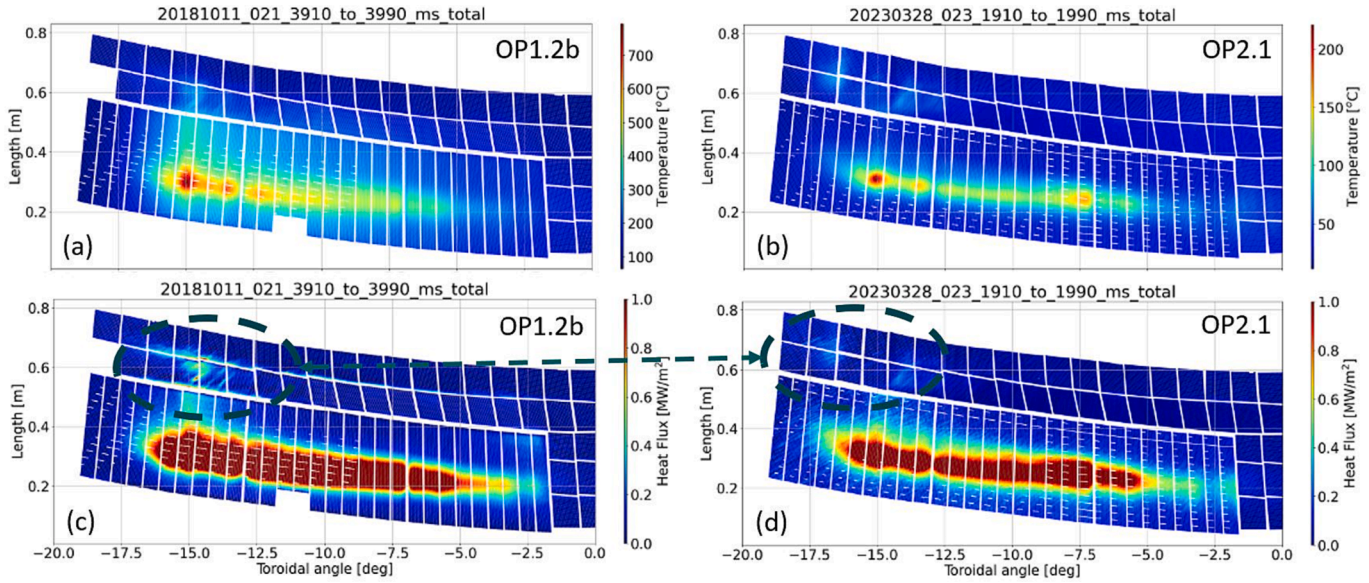

Fig. 3. Comparison of surface temperature and heat load patterns for the different baffle designs as used in OP1.2b and OP2.1 experiment campaigns.

the corresponding sputtering yield for triply charged carbon ions with a Maxwellian energy distribution is $Y_{C3+\rightarrow W} \simeq 9{\cdot}10^{-2}$ [11]. The concentration of the two plasma species must satisfy the quasineutrality condition in the plasma $f_{H+} + q_{C3+} \cdot f_C = f_{H+} + 3\,f_C = 1$. With an estimated carbon concentration of about $f_{C3+} = 3\%$ we obtain $f_{H+} = 0.91$. With a convective heat load of $P_{load} = 0.25$ MW/m^2 and a power transmission factor of about $\gamma_E \approx 8$, for a given electron temperature T_e and angle of incidence of the magnetic field lines ($\alpha \approx 7^\circ$ at the baffle position BM1v), the corresponding electron density is

$$n_e = \frac{P_{load}}{\gamma_E c_s k T_e \sin\alpha} \tag{3}$$

For example, with $T_e = 30$ eV at the sheath entrance we have in case of a hydrogen plasma $n_e = 1.0{\cdot}10^{18}$ m^{-3}; with $T_e = 50$ eV the electron density is $n_e = 4.6{\cdot}10^{17}$ m^{-3}; and with $T_e = 5$ eV, $n_e = 1.5{\cdot}10^{19}$ m^{-3} - for the same power load. The resulting erosion flux density is given by Eq. (2)

$$\Gamma_{H^+,C^{3+}\rightarrow W} = (f_{H^+} Y_{H\rightarrow W} + f_{C^{3+}} Y_{C^{3+}\rightarrow W}) n_e c_s \sin\alpha = 1.7 \bullet 10^{19}\ \text{atoms}/(m^2\text{s}) \tag{4}$$

for $T_e = 30$ eV, $n_e = 1.0 \times 10^{18}$ m^{-3}. The influx of tungsten atoms is

$$\Gamma^W_{ero/ions} = \Gamma_{H^+,C^{3+}\rightarrow W} S_{W-tiles} = 7 \bullet 10^{18}\ \text{atoms/s} \tag{5}$$

Here, an area of 'plasma-facing tungsten' material $S_{\text{W-tiles}} = 40 \times 0.1$ m $\times$ 0.1 m $\simeq 0.4$ m^2 is taken (40 tiles on the baffle modules BM1v in all 10 divertor units).

In addition to the erosion by plasma ions as estimated above, the sputtering of the tungsten surfaces by energetic charge-exchange neutrals must also be considered. Typical values for the flux of energetic neutrals are $\Gamma_{cx} \approx 1{\cdot}10^{19} - 5{\cdot}10^{19}$ neutrals/(m^2 s) [24]. Taking the sputtering yield $Y_{H^\circ\rightarrow W} = 1{\cdot}10^{-4}$ (for $E_{H^\circ} = 700$ eV) [25], we obtain a rather negligible erosion flux of tungsten impurities

$$\Gamma^W_{ero/cx} = \Gamma_{cx} Y_{H^\circ\rightarrow W} S_{W-tiles/wall} = 1.2 \bullet 10^{16}\ \text{atoms/s} \tag{6}$$

Here, an area of 'plasma-facing tungsten' material $S_{W\text{-}tiles/wall} = 240 \times 0.1$ m $\times$ 0.1 m $\simeq 2.4$ m^2 is considered (200 tiles at the heat shield, 40 tiles at the baffle modules BM1v in all 10 divertor units). It should be noted that convective loads on the heat shield surfaces, i.e. direct impact of plasma ions, are not expected, whereas such loads occurred on the baffle modules during the plasma experiments.

The tungsten tiles installed at the baffle module BM1v (see Sect. 2.2) are part of the NBI beam dump area in the plasma vessel module 2. Eight tiles (4 in each divertor unit in half modules 20 and 21) have an area of $S_{W\text{-}tiles/NBI\ dump} = 8 \times 0.1$ m $\times$ 0.1 m $\simeq 0.08$ m^2. With a maximum heat flux density $P_{NBI} = 16$ MW/m^2, we obtain a particle flux density of hydrogen neutrals $\Gamma_{H^\circ\rightarrow W} = 1.8{\cdot}10^{21}H^\circ$/(m^{2}s) for $E_{H^\circ} = 55$ keV. The sputtering yield of tungsten bombarded by hydrogen with this energy of 55 keV is about $Y_{H^\circ\rightarrow W} = 1{\cdot}10^{-3}$ [25]. The resulting erosion flux density is given by

$$\Gamma^W_{ero/NBI} = \Gamma_H Y_{H^\circ\rightarrow W} S_{W-tiles/NBI-dump} = 1.44 \bullet 10^{17}\ \text{atoms/s} \tag{7}$$

Comparing the erosion fluxes due to the different processes (see Eqs. (5–7)), erosion by plasma ions is the major contributor. Melting due to abnormal events, such as those described in Sect. 2.2, is not considered here. Surface temperatures well above 1000 °C must be avoided during plasma operation.

If the impurity retention in the divertor is neglected, the concentration of tungsten ions in the central plasma can be roughly estimated by using the following simple relationship [26]

$$f_W = \frac{\lambda_{iz} \Gamma^W_{ero}}{n_e^{core} D_{perp} S_{pl}} \tag{8}$$

With the following set of parameters: ionization length $\lambda_{iz} = 0.003$ m at the separatrix, $n_e^{core} = 10^{20}$ m^{-3}, cross-field diffusion coefficient $D_{perp} = 1$ m^2/s, $S_{pl} = 4\pi\,(2\,a\,R) = 4\pi\,(2 \times 0.53\text{ m} \times 5.5\text{ m}) = 115$ m^2 we obtain a tungsten core concentration of about $f_W = 1.8{\cdot}10^{-6}$ for an influx of tungsten atoms of $\Gamma_{\text{influx}} = 7.0{\cdot}10^{18}$ [atoms/s] ($T_e = 30$ eV, $n_e = 1.0{\cdot}10^{18}$ m^{-3}, $f_{C3+} = 3\%$ according to Eq. (5)). This value ($f_W = 1.8{\cdot}10^{-6}$) is one order of magnitude lower than the critical value, where the core plasma performance is compromised due to increased radiation losses. It should be noted that the additional effects such as impurity screening in the edge plasma as well as the formation of mixed layers (see Sect. 3.2) will contribute to the reduction of the tungsten influx to the confined region and thus to a correspondingly lower core concentration.

It is interesting to note that using this model, an increase in P_{load} does not lead to an increase in f_W, if the electron temperature is held constant, since the ionization length λ_{iz} is inversely proportional to the electron density. An increase in n_e due to an increase in P_{load} according to Eq. (3) leads to a corresponding decrease in the ionization length and a resulting unchanged core impurity concentration according to Eq. (8).

Core/edge spectroscopy for tungsten

Using Tracer-Encapsulated Solid Pellets (TESPELs) [27] with a defined amount of tungsten material, special experiments were performed in OP2.1 to calibrate the HEXOS VUV spectrometer [28]. Good results were obtained with relatively small amounts of tungsten: for a TESPEL with $0.65{\cdot}10^{17}$ W atoms (W7-X program number XP_20230315.21) and for another TESPEL with $1.3{\cdot}10^{17}$ W atoms (W7-X program number XP_20230315.24). The injections of TESPELs with a larger amounts of tungsten material ($2.5{\cdot}10^{17}$ and $5.5{\cdot}10^{17}$ W atoms) have caused too much disturbance due to rapidly increasing radiation losses shortly after the injection of the heavier TESPELs with large excursions of the core plasma parameters. For these experiments, discharges with 4 MW ECRH heating power, no NBI heating and with line averaged densities of $5{\cdot}10^{19}$ m^{-2} were selected. In a preliminary analysis of the plasma profiles obtained with the Thomson scattering system [29] the following plasma parameters on axis were obtained: for XP_20230315.21 $n_{e,\mathrm{core}} = 4.5{\cdot}10^{19}$ m^{-3}, $T_{e,core} = 3.0$ keV; for XP_20230315.24 $n_{e,\mathrm{core}} = 4.0{\cdot}10^{19}$ m^{-3}, $T_{e,core} = 3.0$ keV. Together with the measurements of the radiation losses during the TESPEL injection using the bolometer diagnostic [30], tungsten core concentration of $f_W = 3{\cdot}10^{-5}$ for XP_20230315.21 with $0.65{\cdot}10^{17}$ W atoms and $f_W = 8.7{\cdot}10^{-5}$ for XP_20230315.24 with $1.3{\cdot}10^{17}$ W atoms are calculated. In this assessment, the cooling rates for tungsten are taken from [31]. By analysing the quasi-continuum line emission of tungsten with charge states up to + 45 in the wavelength range from 4.5 nm to 7 nm, a lower detection limit of the HEXOS spectrometer for tungsten in the core plasma could be defined (for these plasma parameters), which is in the order of $f_{W,limit} = 6.7{\cdot}10^{-7}$.

Comparing this detection limit with the calculated value of $f_W = 1.8{\cdot}10^{-6}$ (see Sect. 3.1, Eq. (8)), and ignoring the associated uncertainties, one could conclude that the HEXOS core spectroscopy is sensitive enough to detect tungsten being emitted from the tungsten baffle tiles, at least under conditions of larger heat/particle loads on these areas. Fig. 4 shows an overview of the tungsten monitoring by the HEXOS diagnostic system during the OP2.1 campaign. As part of the safe operation monitoring, the readings from this spectroscopy were evaluated during the experiment to make changes in the planned experiment operation or parameter changes, if necessary. An increased emission of tungsten impurities was observed during the planned injections of TESPELs as well as during the laser blow-off experiments. In addition, there were incidents during manipulator use (cases B, D, E in Fig. 4). Partly due to the fact that massive molybdenum was introduced by the manipulator, which also led to an intensity increase in the observed wavelength range (case E). Case C showed a W emission and case F a (W + Fe) emission from an unidentified source. In case A, the discharge was interrupted by the interlock system due to excessive stray radiation.

What about the plasma edge spectroscopy [32]? During OP2.1, considerable efforts were devoted to tungsten spectroscopy in the visible range of light emission. In particular, the WI line at 400.9 nm was regularly monitored using a special overview fiber. Its viewing cone (full angle 25°, 1.8 m lens-baffle distance) was adjusted to look at the center of the four W tiles on the baffle module BM1v of the lower divertor unit in plasma vessel module 3 with the AEF30 viewing port, covering almost the entire baffle module. To increase the sensitivity and to avoid count overflow from adjacent channels on the CCD detector this fiber was connected to its own spectrometer at the end of the campaign. It was estimated that a photon flux of $I_{ph/detect.-limit} = 5{\cdot}10^{15}$ photons/(m^2 sr s) represents the lower detection limit. With an inverse photon efficiency (so-called S/XB-value) of about S/XB = 30 [33] for an electron temperature of T_e = 30 eV, the influx of tungsten atoms required for detection can be estimated with $S_{W\text{-}tiles} = 4 \times 0.1\ \mathrm{m} \times 0.1\ \mathrm{m} \simeq 0.04\ \mathrm{m}^2$ in one baffle unit BM1v as

$$\Gamma^{W}_{ero/detect.-limit} = 4\pi\, I_{ph/detect.-limit}(S/XB)S_{W-tiles} = 7.5 \bullet 10^{16}\ \mathrm{atoms/s} \qquad (9)$$

which is well below the calculated influx of tungsten eroded by plasma ions including carbon impurities according to Eq. (5). As confirmed by measurements in CTH and DIII-D, near-neutral charge states of W predicted to radiate strongly in the UV region, lines with strong emission are at 255.13 nm and 265.65 nm for WI. The WII lines at 364.14, 265.80 nm, and 257.14 nm could be used to evaluate the redeposition of singly charged tungsten ionized near the emission point. However, with the current setup of edge spectroscopy at W7-X, this wavelength range is not yet available.

During the observed arcing (XP_20221207.58, as described in Sect. 2.1) a strong W signal was seen with HEXOS, but not in the plasma edge by the visible spectroscopy. The position of the tungsten emission was outside the field of view of the corresponding diagnostics, the ablation of the clusters and the subsequent ionization also took place inside the separatrix, but even in the cooling phase of the collapsing plasma, the low charged tungsten ions and neutral tungsten atoms produced during recombination were not detected by the plasma edge spectroscopy with

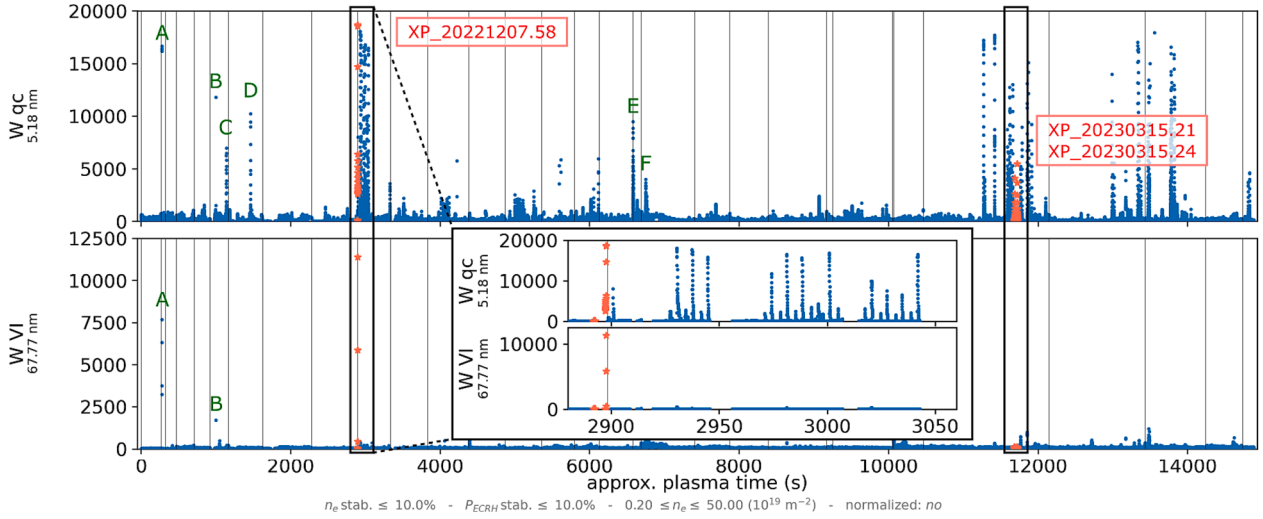

Fig. 4. Measurement of the quasi-continuum emission of tungsten impurities at one wavelength (Wqc) and of the W VI line emission at about 68 nm during the OP2.1 campaign in the time period from November 8, 2022 to March 30, 2023. Strong emission above the noise level was observed during W-TESPEL injection, e.g. in XP_20230315.21 and 0.24, as well as during the fast plasma collapse induced by tungsten cluster emission in XP_20221207.58, see section 2.1. Special events with higher emission are indicated: A (XP_20221109.11), B (XP_20221130.16), C (XP_20221130.39), D (XP_20221201.36), E (XP_20230131.05), F (XP_20230209.10).

a signal higher than the background noise level.

To summarize the experimental findings, tungsten was not detected spectroscopically during normal plasma operation in OP2.1, neither in the visible range at the plasma edge nor with the HEXOS VUV spectrometer monitoring the core plasma even at higher loads on the tungsten baffle tiles - despite sufficient sensitivity as described above. What could be the reason for this? The erosion of material exposed to a plasma containing impurities such as carbon shows a complicated nonlinear behavior [34]. In particular, at low plasma temperatures (with low erosion) and high impurity concentrations (leading to high deposition fluxes), the impurity material is deposited during the bombardment; in this case carbon erodes from other PFCs in the device and is transported/migrated due to ionization and transport processes in the plasma. Higher concentrations of carbon impurities in the plasma (starting from $f_{C3+} >$ 2%), will lead to the formation of carbon layers that protect the underlying tungsten material, thus largely reducing the emitted tungsten influx compared to the values as estimated in Sect. 3.1. Such thick deposits of several micrometers thickness have been observed after OP1.2 on the (graphite) tiles of the BM1v baffle modules [9,10]. The observed high emissivity values of about 0.7 for the tungsten material tiles, to be taken by evaluating the IR thermography data (as reported in Sect. 2.2), also point to the existence of carbon layers on the tungsten surface. For pure tungsten, emissivity values in the range of 0.1 would be expected.

This hypothesis was confirmed after access to the plasma vessel was established in mid-July 2023. During the visual inspection of the PFCs, thick deposits were observed in particular on the baffle areas with the installed tungsten tiles, see Fig. 5. In some locations, even weakly adhering flakes have been detached. The peeling of the micrometer thick layers was supported by the absorption of humidity after venting the plasma vessel. Some of these tiles will be replaced for ex-situ surface analysis with the expectation of finding the known material composition including carbon, hydrogen, oxygen, boron and metal atoms [9,10].

Summary and outlook

As part of the transition to reactor-relevant materials for the plasma facing components in W7-X, selected areas of the inner heat shield and the baffle, where thermal overloads had been observed in previous experiment campaigns, were equipped with tungsten-coated graphite tiles on the heat shield (Sect. 2.1) and with pure metal tiles in the baffle areas (Sect. 2.2).

It must be emphasized that the transition to metal PFCs should begin with the complete removal or coating of the carbon tiles on the heat shield and baffle modules, before the divertor itself should be replaced by a tungsten divertor – with favorable geometry modifications appropriate for improved exhaust and sufficient thermal load capabilities. The gradual increase of the tungsten coverage of the baffle and heat shield areas provides the opportunity to study the effect of tungsten erosion, transport and possible accumulation on the overall plasma performance already in the experiment campaigns of OP2. In OP2.1, high plasma performance could be achieved with the installed tungsten PFCs, tungsten accumulation did not occur – also due to the still limited tungsten surface and the correspondingly small associated tungsten influxes (Sect. 3). In addition, the deposition of carbon as an intrinsic impurity in W7-X prevented the erosion of tungsten. Therefore, no spectroscopic evidence could be obtained during the whole campaign under normal plasma conditions, neither by core spectroscopy nor by edge spectroscopy in the visible range. However, it was also shown how destructively emitted tungsten can limit the plasma operation if, for example, operating errors in the use of the plasma heating systems (Sect. 2.1) lead to

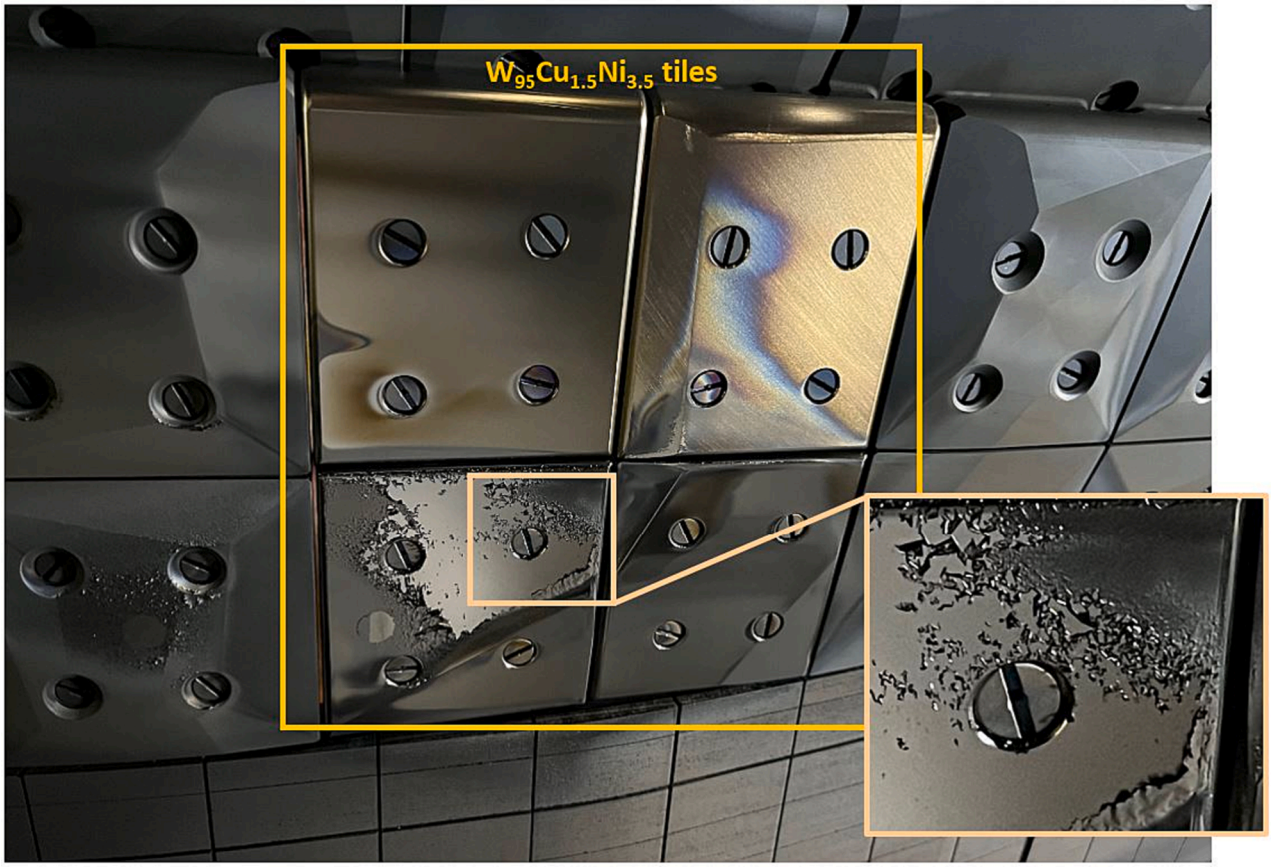

Fig. 5. View of the BM1v baffle module belonging to the lower divertor unit in the plasma vessel module 3 with four W95Ni3.5Cu1.5 tiles (indicated by the yellow rectangle). This photo was taken during the visual inspection after the access to the plasma vessel was granted. Thick deposits are shown forming loosely bounded flakes.

local overloading or arcing, which can then result in the emission of larger amounts of tungsten that terminate the plasma discharge.

To improve plasma edge spectroscopy for tungsten monitoring, the need for a spectrometer system operating in the UV range down to 250 nm was identified, which would also require an appropriate fiber connection with sufficient UV transmission.

It was demonstrated that the geometrical changes made to the modified baffle tiles (Sect. 2.2) resulted in the predicted reductions of heat loads, especially when using the high-mirror configuration. The calculations were thus confirmed, giving confidence in the tools developed for the further design of the PFCs, including the design of the new tungsten divertor. In preparation for the upcoming campaigns, more and more graphite tiles from the heat shield and baffle areas will be replaced by tungsten-coated tiles to increase the tungsten area, in order to prove the compatibility of tungsten PFCs with high-performance operation in the stellarator experiment W7-X.

CRediT authorship contribution statement

Dirk Naujoks: Conceptualization, Methodology, Project administration, Writing – original draft, Writing – review & editing. **Chandra-Prakash Dhard:** Conceptualization, Project administration, Writing – review & editing. **Yuhe Feng:** Conceptualization, Investigation, Writing – review & editing. **Yu Gao:** Investigation. **Torsten Stange:** Conceptualization, Methodology, Project administration, Investigation. **Birger Buttenschön:** Investigation. **Sebastijan Brezinsek:** Conceptualization, Methodology, Investigation. **Andreas Dinklage:** Investigation. **David Ennis:** Investigation. **Joris Fellinger:** Conceptualization, Methodology. **Eric Flom:** Investigation. **Dorothea Gradic:** Investigation. **Eduard Grigore:** Investigation. **Dirk Hartmann:** Conceptualization. **Frederik Henke:** Investigation. **Marcin Jakubowski:** Conceptualization. **Amit Kharwandikar:** Investigation. **Petra Kornejew:** Investigation. **Maciej Krychowiak:** Conceptualization, Investigation. **Matej Mayer:** Conceptualization, Methodology, Writing – review & editing. **Paul McNeely:** Conceptualization. **Daniel Medina:** Investigation. **Rudolf Neu:** Conceptualization, Methodology, Writing – review & editing. **Cristian Ruset:** Conceptualization. **Naoki Tamura:** Investigation. **Erhui Wang:** Investigation. **Thomas Wegner:** Investigation. **Daihong Zhang:** Investigation.

Declaration of Competing Interest

The authors declare that they have no known competing financial interests or personal relationships that could have appeared to influence the work reported in this paper.

Data availability

Data will be made available on request.

Acknowledgement

This work has been carried out within the framework of the EUROfusion Consortium, funded by the European Union via the Euratom Research and Training Programme (Grant Agreement No 101052200 — EUROfusion). Views and opinions expressed are however those of the author(s) only and do not necessarily reflect those of the European Union or the European Commission. Neither the European Union nor the European Commission can be held responsible for them.

References

[1] R.C. Wolf, W7-X Team, Major results from the first plasma campaign of the Wendelstein 7-X stellarator, Nuclear Fusion 57 (2017), 102020.
[2] T. Sunn Pedersen, R. König, M. Krychowiak, M. Jakubowski, J. Baldzuhn, S. Bozhenkov, G. Fuchert, A. Langenberg, H. Niemann, D. Zhang, K. Rahbarnia, H.-S. Bosch, Y. Kazakov, S. Brezinsek, Y. Gao, N. Pablant, W7-X Team, First results from divertor operation in Wendelstein 7-X, Plasma Phys Control. Fusion 61 (2019), 014035.
[3] T. Sunn Pedersen, W7-X Team, Experimental confirmation of efficient island divertor operation and successful neoclassical transport optimization in Wendelstein 7-X, Nuclear Fusion 62 (2022), 042022.
[4] J. Boscary, A. Peacock, R. Stadler, B. Mendelevitch, H. Tittes, J. Tretter, M. Smirnow, C. Li, Actively Water-Cooled Plasma Facing Components of the Wendelstein 7-X Stellarator, Fusion Science and Technology 64 (2) (2013) 263–268.
[5] G. Ehrke, B. Mendelevitch, J. Boscary, C. Li, O. Sellmeier, R. Stadler, P. McNeely, F. Schauer, W7-X Team, Design and manufacturing of the Wendelstein 7-X cryo-vacuum pump, Fusion Eng. Design 146 (2019) 2757–2760.
[6] V. Philipps, D. Kogut, H.G. Esser, G. Sergienko, M. Zlobinski, J.W. Coenen, S. Brezinsek, F. Nachtrodt, A.K. Sanyasi, Deposition and qualification of tungsten coatings produced by plasma deposition in WF6 precursor gas, Physica Scripta T145 (2011), 014030.
[7] D. Naujoks, A. Kharwandikar, V. Haak, T. Sieber, M. Banduch, J. Boscary, Chr. Day, C.P. Dhard, G. Ehrke, J. Fellinger, Y. Feng, Y. Gao, J. Geiger, Yu. Igitkhanov, M. Jakubowski, R. König, T. Kremeyer, R. Neu, G. Schlisio, H. Strobel, T. Sunn Pedersen, Chr. Tantos, J. Tretter, S. Varoutis and the W7-X Team, Divertor concept development for the W7-X stellarator experiment, 4th Technical IAEA Meeting on Divertor Concepts, 7-11 Nov 2022, IAEA Headquarters, Vienna, https://conferences.iaea.org/event/286/contributions/25129/.
[8] J. Fellinger, M. Richou, G. Ehrke, M. Endler, F. Kunkel, D. Naujoks, T.h. Kremeyer, A. Menzel-Barbara, T.h. Sieber, J.-F. Lobsien, R. Neu, J. Tretter, Z. Wang, J.-H. You, H. Greuner, K. Hunger, P. Junghanns, O. Schneider, M. Wirtz, T.h. Loewenhoff, A. Houben, A. Litnovsky, P.-E. Fraysinnes, P. Emonot, S. Roccella, O. Widlund, B. Končar, M. Tekavčič, Tungsten based divertor development for Wendelstein 7-X, Nuclear Materials and Energy 37 (2023) 101506.
[9] C.P. Dhard, S. Brezinsek, M. Mayer, D. Naujoks, S. Masuzaki, D. Zhao, R. Yi, J. Oelmann, K. Schmid, J. Romazanov, C. Pardanaud, M. Kandler, A. K. Kharwandikar, G. Schlisio, O. Volzke, H. Grote, Y. Gao, L. Rudischhauser, A. Goriaev, T. Wauters, A. Kirschner, S. Sereda, E. Wang, M. Rasinski2, T. Dittmar, G. Motojima, D. Hwangbo, S. Kajita, M. Balden, V.V. Burwitz, R. Neu, Ch. Linsmeier, W7-X Team, Plasma-wall interaction studies in W7-X: main results from the recent divertor operations, Physica Scripta 96 (2021), 124059.
[10] S. Brezinsek, C.P. Dhard, M. Jakubowski, R. König, S. Masuzaki, M. Mayer, D. Naujoks, J. Romazanov, K. Schmid, O. Schmitz, D. Zhao, M. Balden, R. Brakel, B. Butterschoen, T. Dittmar, P. Drews, F. Effenberg, S. Elgeti, O. Ford, E. Fortuna-Zalesna, G. Fuchert, Y. Gao, A. Goriaev, A. Hakola, T. Kremeyer, M. Krychowiak, Y. Liang, C.h. Linsmeier, R. Lunsford, G. Motojima, R. Neu, O. Neubauer, J. Oelmann, P. Petersson, M. Rasinski, M. Rubel, S. Sereda, G. Sergienko, T. Sunn Pedersen, T. Vuoriheimo, E. Wang, T. Wauters, V. Winters, M. Zhao, R. Yi, W7-X Team, Plasma–surface interaction in the stellarator W7-X: conclusions drawn from operation with graphite plasma-facing components, Nuclear Fusion 62 (2022), 016006.
[11] D. Naujoks, K. Asmussen, M. Bessenrodt-Weberpals, S. Deschka, R. Dux, W. Engelhardt, A.R. Field, G. Fussmann, J.C. Fuchs, C. Garcia-Rosales, S. Hirsch, P. Ignacz, G. Lieder, K.F. Mast, R. Neu, R. Radtke, J. Roth, U. Wenzel, Tungsten as target material in fusion devices, Nuclear Fusion 36 (1996) 671.
[12] R. Neu, A. Kallenbach, M. Balden, V. Bobkov, J.W. Coenen, R. Drube, R. Dux, H. Greuner, A. Herrmann, J. Hobirk, H. Höhnle, K. Krieger, M. Kočan, P. Lang, T. Lunt, H. Maier, M. Mayer, H.W. Müller, S. Potzel, T. Pütterich, J. Rapp, V. Rohde, F. Ryter, P.A. Schneider, J. Schweinzer, M. Sertoli, J. Stober, W. Suttrop, K. Sugiyama, G. van Rooij, M. Wischmeier, ASDEX Upgrade Team, Overview on plasma operation with a full tungsten wall in ASDEX Upgrade, Journal of Nuclear Materials 438 (2013) S34–S41.
[13] R. Neu, H. Maier, M. Balden, S. Elgeti, H. Gietl, H. Greuner, A. Herrmann, A. Houben, V. Rohde, B. Sieglin, I. Zammuto, ASDEX Upgrade Team, Investigations on tungsten heavy alloys for use as plasma facing material, Fusion Engineering and Design 124 (2017) 450–454.
[14] C. P. Dhard, S. Masuzaki, D. Naujoks, R. Neu, D. Nagata, H. Greuner and K. Hunger, Exposure of tungsten heavy alloys at high thermal loads in GLADIS and LHD, contribution to the PFMC19 (2023), paper is under submission to the Journal of Nuclear Materials and Energy (2023).
[15] H.P. Laqua, J. Baldzuhn, H. Braune, S. Bozhenkov, K. Brunner, M. Hirsch, U. Hoefel, J. Knauer, A. Langenberg, S. Marsen, D. Moseev, E. Pasch, K. Rahbarnia, T. Stange, R.C. Wolf, N. Pablant, O. Grulke, W7-X Team, High-performance ECRH at W7-X: experience and perspectives, Nuclear Fusion 61 (10) (2021) 106005.
[16] C. Ruset, E. Grigore, H. Maier, R. Neu, H. Greuner, M. Mayer, G. Matthews, Development of W coatings for fusion applications, Fusion Engineering and Design 86 (9-11) (2011) 1677–1680.
[17] R. Neu, R. Dux, A. Geier, A. Kallenbach, R. Pugno, V. Rohde, D. Bolshukhin, J. C. Fuchs, O. Gehre, O. Gruber, J. Hobirk, M. Kaufmann, K. Krieger, M. Laux, C. Maggi, H. Murmann, J. Neuhauser, F. Ryter, A.C.C. Sips, A. Stäbler, J. Stober, W. Suttrop, H. Zohm, T.A.U. Team, Zohm and the ASDEX Upgrade Team, Impurity behaviour in the ASDEX Upgrade divertor tokamak with large area tungsten walls, Plasma Phys. Control. Fusion 44 (6) (2002) 811–826.
[18] Y. Gao, Y. Feng, M. Jakubowski, J. Geiger, M. Endler, C.P. Dhard, C. Biedermann, D. Naujoks, T.S. Pedersen, R. König, P. Drewelow, F. Pisano, A. Puig Sitjes, H. Niemann, S. Bozhenkov, S. Lazerson, M. Otte, J. Fellinger, J. Zhu, M. Krychowiak, D. Zhang, B. Cannas, Y. Suzuki, W7-X Team, Understanding baffle overloads observed in high-mirror configuration on Wendelstein 7-X, Nuclear Fusion 60 (2020), 096012.
[19] Y. Gao, Y. Feng, M. Endler, M. Jakubowski, J. Geiger, S. Bozhenkov, A. Puig Sitjes, F. Pisano, C.P. Dhard, D. Naujoks, M. Krychowiak, M. Otte, R. König, D. Zhang,

G. Schlisio, U. Wenzel, T.S. Pedersen, W7-X Team, Improvement in the simulation tools for heat distribution predictions and control of baffle and middle divertor loads in Wendelstein 7-X, Nuclear Fusion 63 (2023), 026031.
[20] S.A. Lazerson, O. Ford, S. Äkaslompolö, S. Bozhenkov, C. Slaby, L. Vanó, A. Spanier, P. McNeely, N. Rust, D. Hartmann, P. Poloskei, B. Buttenschön, R. Burhenn, N. Tamura, R. Bussiahn, T. Wegner, M. Drevlak, Y. Turkin, K. Ogawa, J. Knauer, K.J. Brunner, E. Pasch, M. Beurskens, H. Damm, G. Fuchert, P. Nelde, E. Scott, N. Pablant, A. Langenberg, P. Traverso, P. Valson, U. Hergenhahn, A. Pavone, K. Rahbarnia, T. Andreeva, J. Schilling, C. Brandt, U. Neuner, H. Thomsen, N. Chaudhary, U. Höfel, T. Stange, G. Weir, N. Marushchenko, M. Jakubowski, A. Ali, Y. Gao, H. Niemann, A. Puig Sitjes, R. Koenig, R. Schroeder, N. den Harder, B. Heinemann, C. Hopf, R. Riedl, R.C. Wolf, W7-X Team, First neutral beam experiments on Wendelstein 7-X, Nuclear Fusion 61 (2021), 096008.
[21] Y. Gao, M.W. Jakubowski, P. Drewelow, F. Pisano, A. Puig Sitjes, H. Niemann, A. Ali, B. Cannas, W7-X Team, Methods for quantitative study of divertor heat loads on W7-X, Nuclear Fusion 59 (6) (2019) 066007.
[22] D. Nicolai, V. Borsuk, P. Drews, O. Grulke, K.P. Hollfeld, T. Krings, Y. Liang, C. h. Linsmeier, O. Neubauer, G. Satheeswaran, B. Schweer, G. Offermanns, W7-X Team, A multi-purpose manipulator system for W7-X as user facility for plasma edge investigation, Fusion Engineering and Design 123 (2017) 960–964.
[23] D. Naujoks, Chapter 12.4 in Plasma-Material Interaction in Controlled Fusion (Springer Series on Atomic, Optical, and Plasma Physics, Vol. 39, Springer Verlag, Berlin, Heidelberg, New York, 2006.
[24] H. Verbeek, J. Stober, D.P. Coster, W. Eckstein, R. Schneider, Interaction of charge exchange neutrals with the main chamber walls of plasma machines, Nuclear Fusion 38 (1998) 1789.
[25] W. Eckstein, C. Garcia-Rosales, J. Roth, W. Ottenberger, Sputtering Data, IPP Report 9/82 (1993).
[26] W. Engelhardt, W. Feneberg, Influence of an ergodic magnetic limiter on the impurity content in a tokamak, Journal of Nuclear Materials 76 & 77 (1978) 518–520.
[27] R. Bussiahn, N. Tamura, K.J. McCarthy, R. Burhenn, H. Hayashi, R. Laube, T. Klinger, LHD Experiment Group, W7-X Team, Tracer-Encapsulated Solid Pellet (TESPEL) injection systemfor Wendelstein 7-X, The Review of Scientific Instruments 89 (2018) 10K112.
[28] B. Buttenschön, R. Burhenn, M. Kubkowska, A. Czarnecka, T. Fornal, N. Krawczyk, D. Zhang, N. Pablant, A. Langenberg, P. Valson, H. Thomsen, W. Biel, J. Aßmann, W7-X Team, Spectroscopic impurity survey in the first operation phase of Wendelstein 7-X, in Proceedings of 43rd EPS Conference on Controlled Fusion and Plasma Physics, Leuven, Belgium, European Physics Society, 2016, Vol. 40A, p. P4.012; available at http://ocs.ciemat.es/EPS2016PAP/pdf/P4.012.pdf.
[29] S.A. Bozhenkov, M. Beurskens, A. Dal Molin, G. Fuchert, E. Pasch, M.R. Stoneking, M. Hirsch, U. Höfel, J. Knauer, J. Svensson, H. Trimino Mora, R.C. Wolf, W7-X Team, The Thomson scattering diagnostic at Wendelstein 7-X and its performance in the first operation phase, Journal of Instrumentation 12 (2017) P10004.
[30] D. Zhang, R. Burhenn, C.D. Beidler, Y. Feng, H. Thomsen, C. Brandt, S. Buller, F. Reimold, P. Hacker, R. Laube, J. Geiger, J.M. García Regaña, H.M. Smith, R. König, L. Giannone, F. Penzel, T. Klinger, J. Baldzuhn, S. Bozhenkov, T. Bräuer, J.K. Brunner, B. Buttenschön, H. Damm, M. Endler, F. Effenberg, G. Fuchert, Y. Gao, M. Jakubowski, J. Knauer, T. Kremeyer, M. Krychowiak, S. Kwak, H. P. Laqua, A. Langenberg, M. Otte, N. Pablant, E. Pasch, K. Rahbarnia, A. Pavone, L. Rudischhauser, J. Svensson, C. Killer, T. Windisch, W7-X Team, Bolometer tomography on Wendelstein 7-X for study of radiation asymmetry, Nuclear Fusion 61 (2021), 116043.
[31] T. Pütterich, R. Neu, R. Dux, A.D. Whiteford, M.G. O'Mullane, H.p., Summers and the ASDEX UpgradeTeam, Calculation and experimental test of the cooling factor of tungsten, Nuclear Fusion 50 (2010), 025012.
[32] O. Neubauer, A. Charl, G. Czymek, Y. Gao, M. Knaup, R. König, M. Krychowiak, H.-T. Lambertz, M. Lennartz, C.h. Linsmeier, G. Satheeswaran, B. Schweer, M. Schülke, S. Sereda, W7-X Team, Endoscopes for observation of plasma-wall interactions in the divertor of Wendelstein 7-X, Fusion Engineering and Design 146, Part A (2019) 19–22.
[33] S. Brezinsek, M. Laengner, J.W. Coenen, M.G. O'Mullane, A. Pospieszczyk, G. Sergienko, U. Samm, Spectroscopic determination of inverse photon efficiencies of W atoms in the scrape-off layer of TEXTOR, Physica Scripta T170 (2017), 014052.
[34] D. Naujoks, W. Eckstein, Non-linear erosion effects in plasma experiments, Journal of Nuclear Materials 230 (1996) 93.